Surface Science 630 (2014) 16–21

Contents lists available at ScienceDirect

Surface Science

journal homepage: www.elsevier.com/locate/susc

Deoxygenation of glycolaldehyde and furfural on Mo_2C/Mo(100)

Jesse R. McManus, John M. Vohs *

Department of Chemical & Biomolecular Engineering, University of Pennsylvania, Philadelphia, PA 19104-6363, USA

ARTICLE INFO

Article history:
Received 3 June 2014
Accepted 24 June 2014
Available online 1 July 2014

Keywords:
Mo_2C
Glycolaldehyde
Furfural
Deoxygenation
TPD
HREELS

ABSTRACT

The desire to produce fuels and chemicals in an energy conscious, environmentally sympathetic approach has motivated considerable research on the use of cellulosic biomass feedstocks. One of the major challenges facing the utilization of biomass is finding effective catalysts for the efficient and selective removal of oxygen from the highly-oxygenated, biomass-derived platform molecules. Herein, a study of the reaction pathways for the biomass-derived platform molecule furfural and biomass-derived sugar model compound glycolaldehyde provides insight into the mechanisms of hydrodeoxygenation (HDO) on a model molybdenum carbide catalyst, Mo_2C/Mo(100). Using temperature programmed desorption (TPD) and high resolution electron energy loss spectroscopy (HREELS), it was found that the Mo_2C/Mo(100) catalyst was active for selective deoxygenation of the aldehyde carbonyl by facilitating adsorption of the aldehyde in an η_2(C,O) bonding configuration. Furthermore, the catalyst showed no appreciable activity for furanic ring hydrogenation, highlighting the promise of relatively inexpensive Mo_2C catalysts for selective HDO chemistry.

1. Introduction

Cellulosic biomass has become an attractive alternative feedstock for the production of fuels and chemicals [1–4]. Since biomass consumes atmospheric CO_2 during growth, its use to produce these fuels and chemicals results in decreased greenhouse gas emissions compared to those produced using traditional fossil fuel resources. The effective use of biomass, however, requires the development of highly efficient catalysts for the transformation of the constituent sugars in cellulose and hemicellulose into more desirable products. In particular, catalysts for hydrodeoxygenation (HDO) are needed to partially reduce the highly oxygenated molecules derived from biomass [4–6]. This need has motivated research into the development of HDO catalysts, from which a range of transition metals and metal alloys containing Pd [7–11], Pt [8,12], Ru [13], Ni [14,15], and Fe [14] have been shown to be active for this class of reaction. While many of these catalysts have appealing properties, improvements in selectivity are still needed and the high cost of those containing precious metals needs to be mitigated [6].

Recently the metal carbides Mo_2C and W_2C have emerged as promising low-cost alternatives to precious metal-based HDO catalysts [16–20]. For example, in a recent study Xiong et al. have shown that Mo_2C is a highly selective catalyst for the HDO of furfural ($C_5H_4O_2$), an important intermediate in the upgrading of glucose, to produce 2-methylfuran (C_5H_6O) [20]. In flow reactor studies they obtained a selectivity to 2-methylfuran of ~60% at a relatively low reaction temperature of 423 K. DFT calculations and spectroscopic studies of the interaction of furfural with a model Mo_2C/Mo(110) catalyst indicated that furfural bonds to the surface via the carbonyl group and that this strong interaction helps facilitate hydrogenolysis of the C═O bond.

Motivated by the results of Xiong et al. [20], in the present study we have investigated in additional detail the adsorption and reaction of the oxygenates, glycolaldehyde ($C_2H_4O_2$) and furfural, on a model catalyst consisting of a Mo_2C thin film grown on the surface of a Mo(100) single crystal. Temperature-programmed desorption (TPD) was used to characterize the reaction of these molecules on the Mo_2C/Mo(100) sample and high-resolution electron energy loss spectroscopy (HREELS) was used to identify stable reaction intermediates.

2. Experimental

This investigation was performed using a UHV apparatus described in detail in previous publications [21–24] operated at 2×10^{-10} Torr background pressure. The apparatus was equipped with an SRS RGA200 residual gas analyzer for TPD experiments, an Omicron Auger electron spectrometer for surface composition analysis, an LK technologies HREEL spectrometer for surface vibrational spectroscopy, and a PHI electronics ion gun for sputtering. All TPD data reported herein were collected with a 4 K/s heating rate and have been corrected to account for the cracking pattern of each molecule and the sensitivity of the mass spectrometer. The HREEL spectrometer was operated with a 4 eV beam energy, oriented at 60° with respect to the surface normal, and spectra were collected with an elastic peak of at least 10,000 counts per second and a full-width-half-maximum of 40 cm^{-1}.

The model catalyst consisted of a Mo_2C thin film on a Mo(100) single crystal. The Mo(100) substrate was spot welded to tantalum wires that

* Corresponding author.
E-mail address: Vohs@seas.upenn.edu (J.M. Vohs).

http://dx.doi.org/10.1016/j.susc.2014.06.019
0039-6028/

were connected to an electrical feedthrough on the UHV sample manipulator. The sample was heated resistively and cooled by contacting the ambient side of the electrical feedthrough with liquid N_2. The sample temperature was monitored using a type K thermocouple spot welded to the back of the crystal. The Mo(100) surface was initially cleaned using repeated sputter–anneal cycles consisting of sputtering with 2 kV Ar^+ ion beam followed by annealing at 1100 K. The Mo_2C film was then synthesized using a method similar to that used previously by Schöberl [25] and Farkas and Solymosi [19] which consisted of exposing the Mo(100) surface to 5×10^{-8} Torr of ethylene at 900 K for 10 min. Carbide formation was confirmed via AES spectroscopy, as described in Supplemental information (see Fig. S1) and prescribed by Haas et al. [26].

Glycolaldehyde (Pfaltz and Bauer, dimer, 98%), furfural (Sigma Aldrich, 99%), and 2-methylfuran (Alfa Aesar, 98 + %) were dosed from a heated glass vial attached to a heated, stainless steel manifold that was connected to the main UHV apparatus via a variable leak valve. The UHV side of the leak valve was equipped with a directional dosing tube to enhance the flux of reactant molecules to the sample surface. The enhancement factor relative to that based on the measured pressure while dosing was estimated to be 5× which was determined using CO adsorption on Pt(111). Furfural and 2-methylfuran were dosed at room temperature, while the glycolaldehyde dimer had to be dissociated and dosed at 370 K. The purity of the reagents was confirmed using the quadrupole mass spectrometer.

3. Results

3.1. Glycolaldehyde

Fig. 1 displays TPD data obtained following a 0.35 L exposure of glycolaldehyde on Mo_2C/Mo(100) at 115 K. This exposure was found to be sufficient to saturate the surface with glycolaldehyde as indicated by the emergence of a zeroth-order molecular glycolaldehyde desorption peak at 194 K (glycolaldehyde desorption spectra as a function of dosage are shown in Fig. S2). The desorption products in Fig. 1 can be broken into two regimes: below 550 K where the primary product is ethylene, and above 550 K where CO, CO_2 and H_2 are produced. The relative yields of all the products are listed in Table 1. The ethylene desorption feature which results from deoxygenation of the glycolaldehyde reactant is quite broad and consists of multiple overlapping peaks with the largest features between 350 and 550 K. This product is reaction limited, as ethylene was found to desorb from ethylene-dosed Mo_2C/Mo(100) at 260 K as shown in Fig. 2(c). In addition to the ethylene product, water, formaldehyde, and ethanol desorbed in peaks between 200 and 350 K.

Table 1
Relative product yields during TPD for Mo_2C/Mo(100) saturated with glycolaldehyde.

Product	Relative yield
H_2	1.00
CO	0.76
C_2H_4	0.74
CH_2O	0.46
H_2O	0.42
CH_3CH_2OH	0.28

The second, higher-temperature reaction regime in the TPD of glycolaldehyde occurs above 550 K and only exhibits peaks for H_2 and

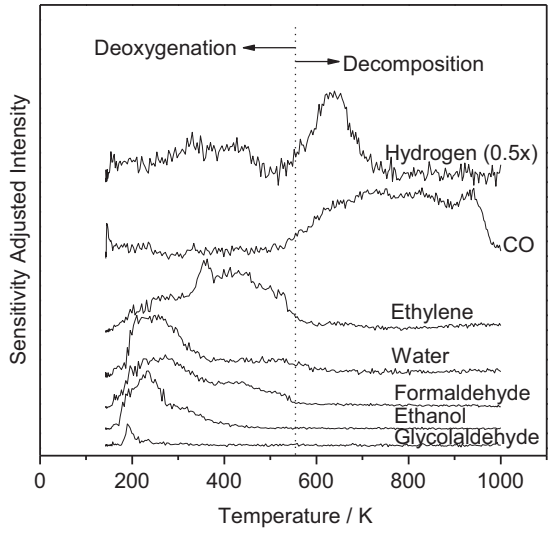

Fig. 1. TPD spectra obtained following a saturation exposure of glycolaldehyde on Mo_2C/Mo(100).

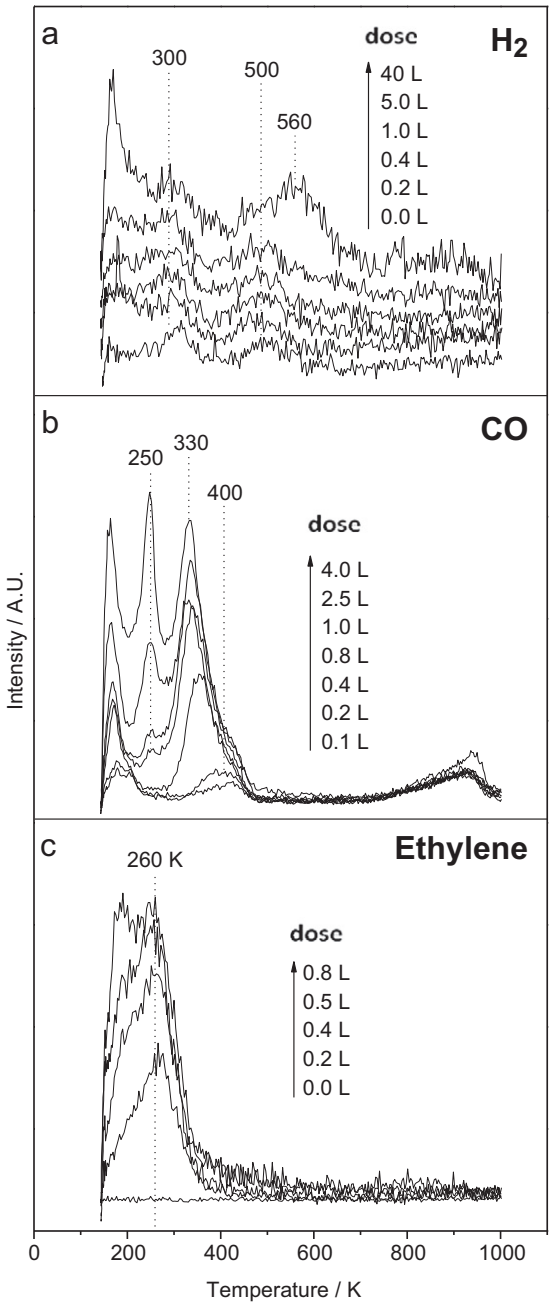

Fig. 2. TPD spectra as a function of dose size for an Mo_2C/Mo(100) surface dosed with (a) H_2, (b) CO, and (c) ethylene.

CO. As shown by the TPD data in Fig. 2(a) and (b) for samples dosed with H_2 and CO, respectively, these molecules desorb from Mo_2C/Mo(100) below 550 K; thus, the high-temperature products from the glycolaldehyde-dosed Mo_2C/Mo(100) surface must also be reaction limited.

HREELS data for a saturation glycolaldehyde exposure on Mo_2C/Mo(100) as a function of temperature are provided in Fig. 3. At 115 K, the surface species exhibit energy-loss peaks characteristic of molecular glycolaldehyde [22], including a ν(OH) stretch at 3360 cm^{-1}, a distinct aldehyde ν(C═O) stretch at 1715 cm^{-1}, and an alcohol ν(CO) stretch at 1075 cm^{-1}. Complete peak assignments along with a comparison to the vibrational spectra of gaseous glycolaldehyde [27] and glycolaldehyde adsorbed on Pd(111) [22] and Pt(111) [21] are given in Table 2. Upon heating from 115 K to 180 K, a number of changes occur in the HREEL spectrum indicating alteration in the bonding configuration of the adsorbed glycolaldehyde. In particular, there is a dramatic decrease in the intensity of the peaks at 745 and 850 cm^{-1}, the near disappearance of the ν(C═O) stretch at 1715 cm^{-1}, and a large decrease in the intensity of the broad ν(OH) stretch at 3360 cm^{-1}. A decrease in the intensity of the peaks between 600 and 850 cm^{-1} has previously been reported in studies of the interaction of glycolaldehyde with Pt(111) [21,24], Pd(111) [22], and Zn/Pt(111) [21], and has been attributed to bonding of the glycolaldehyde to the surface via the C═O and OH groups which constrains the molecular backbone causing a change in the intensity of the δ(CCO) (745 cm^{-1}) and ν(CC) (850 cm^{-1}) modes. The large decrease in the intensity of the ν(OH) stretch (3360 cm^{-1}) indicates dissociation of the OH group, which may also contribute to a decrease in the intensity of the 745 cm^{-1} peak that is partially due to a τ(OH) mode. The disappearance of the ν(C═O) stretch at 1715 cm^{-1} is consistent with transition from a free carbonyl group to one that is bound to the surface. Bonding of at least a portion of the carbonyl groups in an η_1 configuration, where interaction with the surface occurs via the lone pair electrons on the oxygen, is indicated by the small characteristic ν(C═O) stretch of this species at 1685 cm^{-1} [28]. Note, however, that η_2 bonding of carbonyl groups where both the C and the O interact with the surface cannot be ruled out. The ν(C–O) stretch for this configuration would be expected between 1200 and 1400 cm^{-1} [29,30] which overlaps with the CH and CH_2 deformation modes. This mode would also be relatively weak since this configuration requires the carbonyl group to be situated nearly parallel to the surface, decreasing the cross section for excitation.

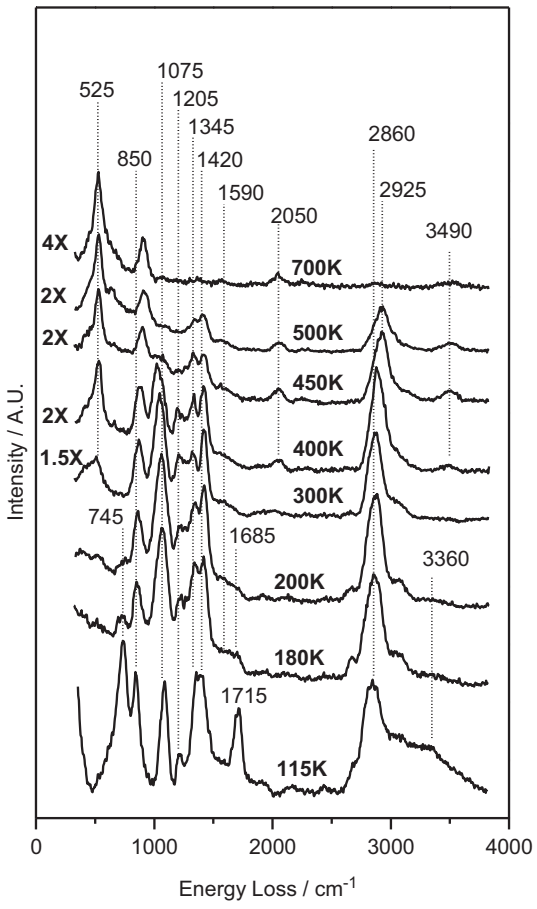

Fig. 3. HREEL spectra as a function of temperature for a Mo_2C/Mo(100) sample dosed with 0.3 L glycolaldehyde at 115 K.

Table 2
Vibrational mode assignments for glycolaldehyde dosed on various surfaces.

Mode	Frequency (cm^{-1})			
	IR (vapor) [27]	Pd(111) [22]	Pt(111) [21]	Mo_2C/Mo(100)
ν(OH)	3549	3315	3377	3360
ν(CH)	2881	2827	2901	2860
$\nu(CH_2)$	2881	2827	2901	2860
ν(C═O)	1754	1715	1715	1715
η_1 ν(C═O)	–	–	1610	1685
δ(CH), $\delta(CH_2)$	1425	1390	1421	1345, 1420
$\rho(CH_2)$	–	–	1173	1205
ν(CO)	1112	1057	1091	1075
ν(CC)	859	880	917	850
γ(CH), τ(OH)	–	775	736	745
δ(CCO), τ(OH)	–	639	620	745
ν(M–C), ν(M–O)	–	–	531	–

ν – stretch, δ – deformation, ρ – rock, γ – wag, and τ – twist.

Upon heating to 300 K, the ν(OH) stretch completely disappears, and a peak at 525 cm^{-1} begins to build in, which is attributable to a surface-adsorbate, Mo–C bond. Additionally, the peak at 1685 cm^{-1} is no longer distinguishable, marking a disappearance of the η_1 bound carbonyl. At 400 K, a new peak emerges at 1020 cm^{-1} which may be due to the ν(CO) mode of an alkoxide species. While this assignment is consistent with the observed dissociation of the hydroxyl group, this peak may also be due to the ν(CC) mode of adsorbed hydrocarbon species that are formed in this temperature range. At 400 K the emergence of surface-bound hydroxyl groups as indicated by a weak ν(OH) peak at 3490 cm^{-1} is also evident. Note that formation of this species implies C–O scission in the adsorbed oxygenate. A small ν(CO) peak at 2050 cm^{-1} is also evident at 400 K, which we attribute to the adsorption of a small amount of CO from the background gas in the vacuum chamber.

Heating to 450 K caused the vibrational spectrum to change sufficiently to preclude a surface intermediate that resembles an intact glycolaldehyde molecule, instead it now resembles a surface hydrocarbon fragment exhibiting only C–H and C–C vibrational modes. In particular, aside from the peaks at 525 cm^{-1} and 915 cm^{-1} (which are also present as the only features at 700 K), the only other peaks due to adsorbed intermediates are $\delta(CH_x)$ and $\rho(CH_x)$ features in the 1300–1450 cm^{-1} range, and a $\nu(CH_x)$ stretch at 2925 cm^{-1}, shifted from the lower temperature glycolaldehyde ν(CH) stretch at 2860 cm^{-1}. These peaks persist to 500 K, but disappear upon heating to 700 K.

3.2. Furfural

Fig. 4 displays TPD results for a Mo_2C/Mo(100) surface dosed with a saturation exposure of furfural, which was determined to be approximately 0.1 L (see Fig. S3). Corresponding relative yields of the various products are listed in Table 3. Similar to the glycolaldehyde TPD in Fig. 1, two separate regimes are apparent for the reaction of furfural. The first occurs at temperatures below 485 K where cleavage of the carbonyl oxygen results in the formation of 2-methylfuran. This product is reaction limited, as molecularly-adsorbed 2-methylfuran desorbs from Mo_2C/Mo(100) at 142 K (see Fig. S4). The hydrogen required for this hydrodeoxygenation pathway likely comes from further decomposition

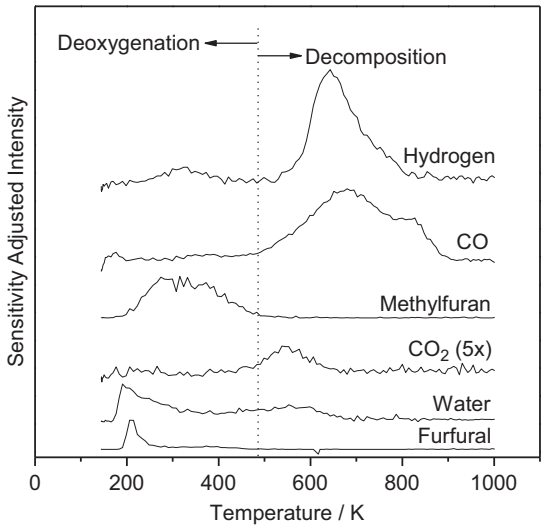

Fig. 4. TPD spectra obtained following a saturation exposure of furfural on Mo_2C/Mo(100).

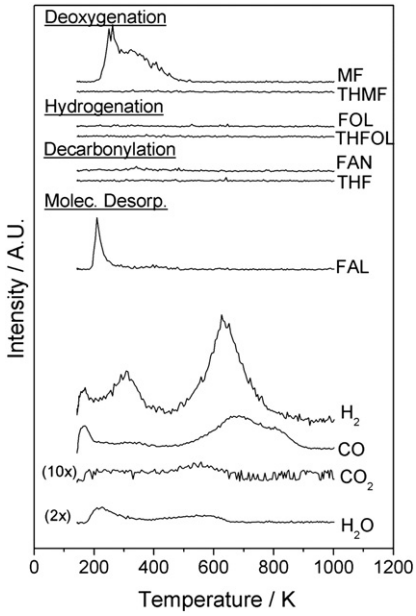

Fig. 5. TPD for a saturation furfural exposure on a Mo_2C/Mo(100) sample that was pre-exposed with 50 L of H_2. MF = methylfuran, THMF = tetrahydrofuran, FOL = furfuryl alcohol, THFOL = tetrahydrofurfuryl alcohol, FAN = furan, THF = tetrahydrofuran, and FAL = furfural.

of a portion of the furfural reactant. The blank H_2 TPD spectrum in Fig. 2(a) demonstrates that a small amount of H_2 adsorbs on the sample from the chamber background and this could also provide some hydrogen for this reaction.

A furfural TPD experiment was also performed with a sample that was intentionally pre-dosed with 50 L of H_2. As shown in Fig. 5 the desorption spectra for this run were essentially the same as those obtained from the sample that was not pre-dosed with H_2. Of particular note is that in both cases products requiring hydrogenation of the ring, such as tetrahydrofuran or tetrahydrofurfuryl alcohol, were not produced. Except for the 2-methylfuran and a small amount of furfural at 210 K, additional furan-based products, such as furfuryl alcohol (FOL) or furan (FAN) were also not detected.

In the second, higher-temperature reaction regime (above 485 K), in a manner similar to that observed for glycolaldehyde (Fig. 4), reaction limited CO and H_2 were the major products resulting from the complete decomposition of adsorbed intermediates. It should be noted that some of the high-temperature CO produced could result from oxidation of the carbide surface.

HREELS data as a function of temperature for a Mo_2C/Mo(100) surface exposed to a saturation dose of furfural are shown in Fig. 6. At 115 K (bottom of Fig. 6(a)), the HREEL spectrum is consistent with the IR and Raman spectra of furfural [31–33] and the HREEL spectrum of molecular furfural adsorbed on Mo_2C/Mo(110) at low temperatures [20]. Peak assignments are tabulated and juxtaposed to relevant IR, Raman and HREELS data in Table 4. Of particular note in this spectrum are the pronounced features indicative of the CHO group, including a ν(C═O) peak at 1650 cm^{-1} and the aldehyde specific ν(CH) peak at 2800 cm^{-1}, as well as an intense ring ν(CH) peak at 3075 cm^{-1}. Upon heating the surface to 200 K, the bonding configuration of the aldehyde group appears to be modified as indicated by changes only in the aldehyde group specific peaks in the spectrum. In particular, the aldehyde ν(C═O) stretch at 1650 cm^{-1} disappears, the aldehyde ν(CH) at 2800 cm^{-1} shifts to 2875 cm^{-1}, and the aldehyde-ring ν(CC) at 500 cm^{-1} is no longer apparent. Because the aldehyde-specific C–H stretch only shifted rather than disappearing, it is likely that the aldehyde functionality remains intact and is bonded to the surface in an η_2(C,O) configuration. The ν(C–O) stretch for this species should be near 1000 cm^{-1} but would be rather weak due to the C–O bond being situated nearly parallel to the surface. Unfortunately, this region of the spectrum is dominated by peaks associated with the furan ring precluding the unambiguous identification of this ν(C–O) stretch. It is also worth noting that there is no shift in the position of the ring breathing mode upon heating from 115 K to 200 K. This peak remains fixed at 1570 cm^{-1} which is also its location in the IR spectrum of the free molecule (see Table 4). This suggests that even though the furan ring is situated parallel to the surface in the η_2(C,O) bonding configuration, it must interact relatively weakly with the surface. This result is consistent with the DFT calculations for the interaction of furfural, furan, and 2-methyl furan with Mo_2C(0001) reported by Xiong et al. [20].

Table 3
Relative product yields during TPD for Mo_2C/Mo(100) saturated with furfural.

Product	Relative yield
H_2	0.99
CO	1.00
H_2O	0.43
C_5H_6O (MF)	0.42
CO_2	0.03

In the transition from 200 to 300 K, there are only minor changes in the HREEL spectrum. Peaks associated with the furan ring persist, including the ring CH peaks at 750 and 3075 cm^{-1} corresponding to the γ(CH) and ν(CH) modes, respectively. Some of the changes include a slight broadening and some alteration in the relative intensities of the peaks at 1350 and 1435 cm^{-1}. As shown in Table 4, these peaks are at least partially due to vibrational modes of the furan ring. Rocking modes associated with the CHO group are also expected in this region as are $-CH_x$ deformations [34–37]. Furthermore, the weak aldehyde ν(CH) stretch at 2875 cm^{-1} in the 200 K spectrum has both increased in intensity and broadened considerably by 300 K. We can only speculate as to the origin of these changes, but together they seem to suggest some alteration in the CHO group. This is consistent with the fact that methylfuran was produced in this temperature range during TPD with furfural-dosed surfaces (see Fig. 4).

Further heating to 470 K produced more substantial changes in the HREEL spectrum of the adsorbed species (see Fig. 6(b)). There are strong indications for the onset of the decomposition of the furan ring including disappearance of the ring γ(OCC) wag at 580 cm^{-1}, a marked decrease in the intensity of the ring γ(CH) wag and χ(CH) scissor modes at 750 and 1205 cm^{-1}, and a dramatic decrease in the originally sharp and intense ring ν(CH) stretch at 3075 cm^{-1}. Furthermore, intensification, shifting and broadening of the $\nu(CH_x)$ and $\delta(CH_x)$ losses suggest a

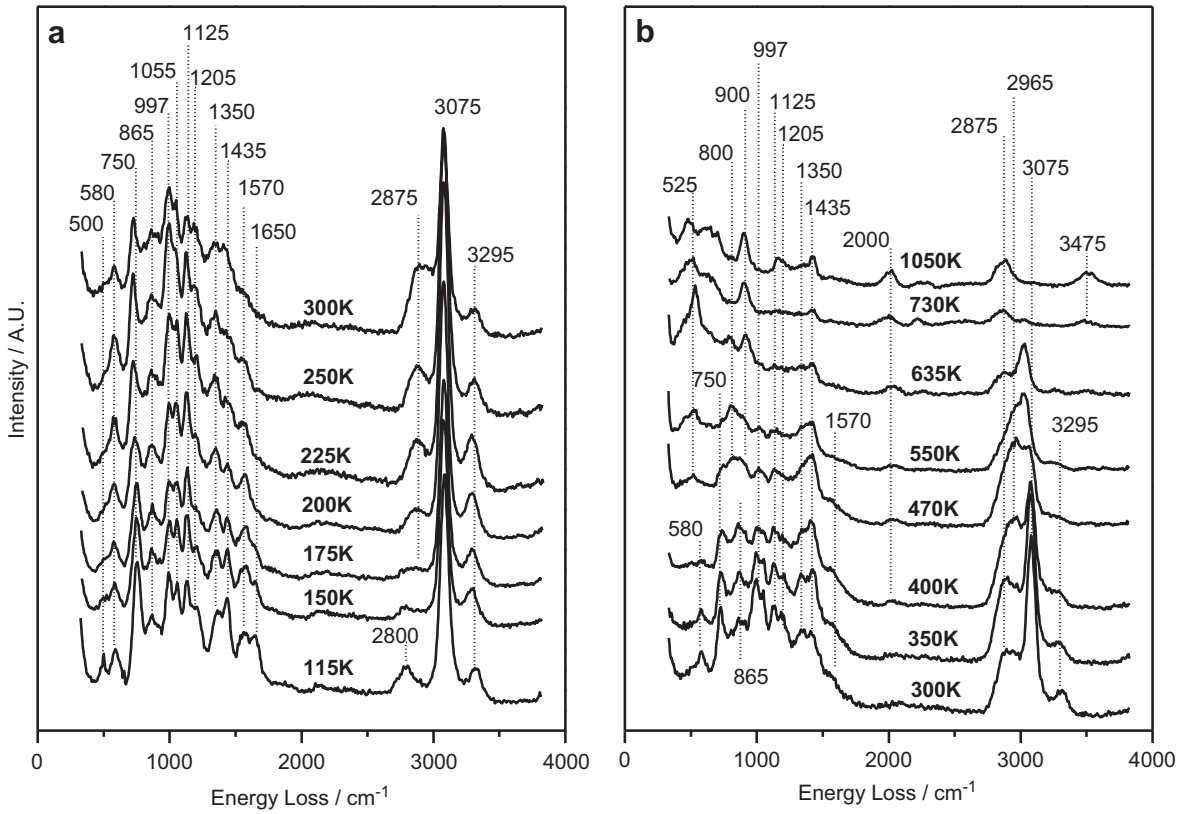

Fig. 6. HREEL spectra as a function of temperature for a Mo_2C/Mo(100) sample dosed with 0.1 L furfural at 115 K, (a) 115–300 K and (b) 300–1050 K.

hydrocarbon surface species. New peaks at 800 and 900 cm^{-1} are likely due to new νCC carbon stretches associated with the hydrocarbon surface species. Continued heating to 550 K and beyond results in decomposition to form adsorbed CO, as evidenced by the characteristic peak at 2000 cm^{-1}.

4. Discussion

The results of this study provide further insight into the reaction of biomass-derived oxygenates on molybdenum carbide surfaces. The TPD data in Figs. 1 and 4 show the production of deoxygenation products, ethanol and ethylene in the case of glycolaldehyde, and methylfuran in the case of furfural, below 500 K. Thus, consistent with Xiong et al.'s [20] previous studies of the reaction of furfural on Mo_2C/Mo(110), the Mo_2C/Mo(100) surface is active for the selective deoxygenation of the carbonyl group in aldehyde containing oxygenates at relatively low temperatures.

The HREELS data provide useful insight into the bonding configuration of adsorbed aldehyde containing oxygenates on Mo_2C/Mo(100) and the mechanism of the deoxygenation reaction. For both adsorbed glycolaldehyde and furfural, bonding to the surface appears to initially occur primarily through the carbonyl group of the aldehyde functionality. At temperatures below ~200 K, the ν(C═O) stretching vibrations, 1715 cm^{-1} for glycolaldehyde and 1650 cm^{-1} for furfural, are consistent

Table 4
Vibrational mode assignments of furfural on various surfaces.

Mode	Frequency (cm^{-1})				
	IR/Raman [31]	Raman [33]	NRS [32]	Mo_2C/Mo(110) [20]	Mo_2C/Mo(100)
ν_{ring}(CH)	3030–3160	3153	–	3091	3075
$\nu_{aldehyde}$(CH)	2813–2858	–	–	2882	2800, 2875
ν(C═O)	1665–1695	1684	1665	1644	1650
Ring breath	1572	–	1570	–	1570
ν(C═C)	1393–1479	1570, 1466	–	1536, 1427	1435
δ_b(OCH)	–	1370, 1157	–	1353, 1136	1350
ρ(CH), χ(CH)	755–885	–	1398, 1464, 1475	–	1350
$\rho_{aldehyde}$(CH)	–	–	1366	–	–
ρ_{as}(CH), χ_{as}(CH)	–	–	1227	1238	1205
ν_{ring}(CO)	–	1025, 930	1156	1028	1125
Ring breath	–	–	1078	–	1055
χ_s(CH)	–	950	1078, 1021	–	997
$\gamma_{aldehyde}$(CH)	–	–	951	–	–
Ring breath	500–630	–	932	866	865
γ_s(CH), γ_{as}(CH) (ring)	–	–	761, 884	758	750
γ_{ring}(OCC)	–	–	595	–	580
ν(CC) (ring-aldehyde)	–	–	508	–	500

s — symmetric, as — asymmetric, b — bend, ν — stretch, δ — deformation, ρ — rock, γ — wag, and χ — scissor.

with an η_1(O) bonding configuration where interaction with the surface occurs via the carbonyl oxygen. In both cases the HREELS data indicate transition to a di-σ η_2(C,O) configuration between 200 and 300 K in which the carbonyl group is nearly parallel to the surface with bonding via both the carbon and oxygen atoms. This conclusion is also consistent with the HREELS and DFT results reported by Xiong et al. [20] for the adsorption of furfural on Mo_2C/Mo(110). The similarity of the results for the Mo_2C/Mo(110) and Mo_2C/Mo(100) surfaces also suggests that the crystallographic orientation does not significantly influence the surface chemistry.

As has previously been reported for both metal alloy surfaces, such as Fe/Ni [14], Zn/Pt [21], and Mo_2C/Mo(110) [20], stabilization of the di-$\sigma\eta_2$(C,O) bonding configuration results in weakening of the carbonyl C – O bond and thereby helps facilitate its cleavage. For glycolaldehyde on Mo_2C/Mo(100), cleavage of this bond occurs between 300 and 400 K as evidenced by the re-emergence of surface-bound hydroxyls upon heating to 400 K (which has also been reported for glycolaldehyde deoxygenation on Zn/Pt(111) surfaces [21]) and the production of ethylene between 300 and 550 K. Similarly for furfural, the increase in intensity and shifting of the aldehyde $\nu(CH_x)$ peak near 2800 cm^{-1} upon heating above 200 K and the production of methylfuran between 200 and 485 K demonstrate carbonyl C – O cleavage in this temperature range.

Additionally it is worth noting that while the Mo_2C/Mo(100) surface is active for hydrodeoxygenation of adsorbed furfural to produce methylfuran, it does not appear to be active for hydrogenation for the furan ring since tetrahydromethylfuran and tetrahydrofurfuryl alcohol were not produced, even when the surface was pre-dosed with H_2. These products are also not observed for the reaction of furfural and H_2 over polycrystalline Mo_2C [20]. These observations are consistent with bonding of the furfural reactant to the Mo_2C/Mo(100) surface primarily via the aldehyde group.

5. Conclusions

This study provides additional insight into the adsorption and reaction of biomass-relevant aldehyde containing oxygenates, glycolaldehyde and furfural, on Mo_2C. Both of these molecules interact with an Mo_2C/Mo(100) surface primarily through the aldehyde functional group. HREELS indicates bonding primarily in an η_1(O) configuration below 200 K with conversion to a di-σ η_2(C,O) configuration upon heating between 200 and 300 K. This bonding configuration results in weakening of the C – O bond in the carbonyl group which appears to play a pivotal role in facilitating its dissociation. While the Mo_2C/Mo(100) surface was active for hydrodeoxygenation of aldoses at the aldehyde functionality, it was inactive for the hydrogenation of the furan ring in furfural. These results further highlight the promise of Mo_2C as a relatively inexpensive, yet highly selective hydrodeoxygenation catalyst for biomass-derived oxygenates.

Acknowledgment

This work was supported as part of the Catalysis Center for Energy Innovation, an Energy Frontier Research Center funded by the U.S. Department of Energy, Office of Science, Office of Basic Energy Sciences under award no. DE-SC0001004.

Appendix A. Supplementary data

Supplementary data to this article can be found online at http://dx.doi.org/10.1016/j.susc.2014.06.019.

References

[1] G.W. Huber, S. Iborra, A. Corma, Chem. Rev. 106 (2006) 4044.
[2] P. Gallezot, Chem. Soc. Rev. 41 (2012) 1538.
[3] M. Stocker, Angew. Chem. Int. Ed. 47 (2008) 9200.
[4] J.N. Chheda, G.W. Huber, J.A. Dumesic, Angew. Chem. Int. Ed. 46 (2007) 7164.
[5] R. Rinaldi, F. Schuth, Energy Environ. Sci. 2 (2009) 610.
[6] S. Dutta, ChemSusChem 5 (2012) 2125.
[7] C. Zhao, Y. Kou, A.A. Lemonidou, X.B. Li, J.A. Lercher, Angew. Chem. Int. Ed. 48 (2009) 3987.
[8] A. Gutierrez, R.K. Kaila, M.L. Honkela, R. Slioor, A.O.I. Krause, Catal. Today 147 (2009) 239.
[9] S. Sitthisa, T. Pham, T. Prasomsri, T. Sooknoi, R.G. Mallinson, D.E. Resasco, J. Catal. 280 (2011) 17.
[10] S.H. Pang, J.W. Medlin, ACS Catal. 1 (2011) 1272.
[11] V. Vorotnikov, G. Mpourmpakis, D.G. Vlachos, ACS Catal. 2 (2012) 2496.
[12] R.M. West, Z.Y. Liu, M. Peter, J.A. Dumesic, ChemSusChem 1 (2008) 417.
[13] L.G. Chen, Y.L. Zhu, H.Y. Zheng, C.H. Zhang, Y.W. Li, Appl. Catal., A 411 (2012) 95.
[14] S. Sitthisa, W. An, D.E. Resasco, J. Catal. 284 (2011) 90.
[15] Y.C. Lin, C.L. Li, H.P. Wan, H.T. Lee, C.F. Liu, Energy Fuels 25 (2011) 890.
[16] A.L. Jongerius, R.W. Gosselink, J. Dijkstra, J.H. Bitter, P.C.A. Bruijnincx, B.M. Weckhuysen, ChemCatChem 5 (2013) 2964.
[17] R.W. Gosselink, D.R. Stellwagen, J.H. Bitter, Angew. Chem. Int. Ed. 52 (2013) 5089.
[18] H. Ren, W.T. Yu, M. Salciccioli, Y. Chen, Y.L. Huang, K. Xiong, D.G. Vlachos, J.G.G. Chen, ChemSusChem 6 (2013) 798.
[19] A.P. Farkas, F. Solymosi, Surf. Sci. 601 (2007) 193.
[20] K. Xiong, W.S. Lee, A. Bhan, J.G. Chen, Chemsuschem (2014), http://dx.doi.org/10.1002/cssc.201.
[21] J.R. McManus, E. Martono, J.M. Vohs, ACS Catal. 3 (2013) 1739.
[22] J.R. McManus, M. Salciccioli, W.T. Yu, D.G. Vlachos, J.G.G. Chen, J.M. Vohs, J. Phys. Chem. C 116 (2012) 18891.
[23] J.R. McManus, J.M. Vohs, Appl. Surf. Sci. 271 (2013) 45.
[24] J.R. McManus, W.T. Yu, M. Salciccioli, D.G. Vlachos, J.G.G. Chen, J.M. Vohs, Surf. Sci. 606 (2012) L91.
[25] T. Schoberl, Surf. Sci. 327 (1995) 285.
[26] T.W. Haas, J.T. Grant, G.J. Dooley, J. Appl. Phys. 43 (1972) 1853.
[27] M. Jetzki, D. Luckhaus, R. Signorell, Can. J. Chem. 82 (2004) 915.
[28] H.B. Zhao, J. Kim, B.E. Koel, Surf. Sci. 538 (2003) 147.
[29] M.A. Henderson, Y. Zhou, J.M. White, J. Am. Chem. Soc. 111 (1989) 1185.
[30] M.A. Henderson, P.L. Radloff, J.M. White, C.A. Mims, J. Phys. Chem. 92 (1988) 4111.
[31] G. Allen, H.J. Bernstein, Can. J. Chem. 33 (1955) 1055.
[32] T.J. Jia, P.W. Li, Z.G. Shang, L. Zhang, T.C. He, Y.J. Mo, J. Mol. Struct. 873 (2008) 1.
[33] T. Kim, R.S. Assary, L.A. Curtiss, C.L. Marshall, P.C. Stair, J. Raman Spectrosc. 42 (2011) 2069.
[34] J.L. Davis, M.A. Barteau, J. Am. Chem. Soc. 111 (1989) 1782.
[35] J.L. Davis, M.A. Barteau, Surf. Sci. 235 (1990) 235.
[36] M.B. Griffin, E.L. Jorgensen, J.W. Medlin, Surf. Sci. 604 (2010) 1558.
[37] O. Skoplyak, M.A. Barteau, J.G.G. Chen, Surf. Sci. 602 (2008) 3578.